IOP Conf. Series: Materials Science and Engineering **1344** (2026) 012042 doi:10.1088/1757-899X/1344/1/012042

Commissioning results of the ESS cryogenic moderator system using helium

H Tatsumoto*, A Horvath, T Vasilopoulos, I Haag, J Arriagada and P Arnold

European Spallation Source (ESS) ERIC, Lund, Sweden.

*E-mail: hideki.tatsumoto@ess.eu

Abstract. At the European Spallation Source, a cryogenic moderator system (CMS) was designed to supply subcooled liquid hydrogen at 17 K with a parahydrogen fraction exceeding 99.5% to each moderator. A flow rate of over 240 g/s is maintained to limit the average temperature rise across the moderator to within 3 K. Heat load is effectively removed via a heat exchanger connected to a 20 K helium refrigeration plant, the Target Moderator Cryoplant (TMCP), with a cooling capacity of 30.3 kW at 15 K. Prior to hydrogen operation, CMS commissioning was carried out using helium, bypassing the moderators. The CMS was successfully cooled down to 17 K utilizing the developed controllers while maintaining a pressure of 0.56 MPa. Performance tests conducted at 17 K confirmed that the CMS met the design specifications. This paper presents detailed performance test results obtained during the preliminary commissioning using helium.

1. Introduction

At the European Spallation Source (ESS), a 5 MW beam of 2.0 GeV proton with a nominal current of 62.5 mA driven by a linear accelerator impacts a rotating tungsten target at a repetition rate of 14 Hz and a pulse length of 2.86 ms. The fast neutrons produced via spallation process are moderated to cold and thermal neutrons by passing through a thermal water pre-moderator and, subsequently, up to two liquid hydrogen moderators [1]. Initially, two hydrogen moderators are installed above the target wheel, with plans to upgrade to four moderators positioned above and below the target in the future. The nuclear heating is estimated to be 6.7 kW for a 5 MW proton beam using two moderators, and 17.2 kW when four moderators are in operation [1].

A cryogenic moderator system (CMS) has been designed to continuously supply subcooled liquid hydrogen at 17 K with a parahydrogen fraction exceeding 99.5% to each moderator, as shown in Fig. 1. A flow rate of 250 g/s is delivered to each moderator to limit the average temperature rise across the moderator within 3 K [2]. For 5-MW proton beam operation, the total heat load of 21.9 kW, which includes a static one of 4.6 kW, is removed via a plate-fin type heat exchanger (HX11) connected to a large-scale 20 K helium refrigeration plant, which is called the Target Moderator Cryoplant (TMCP), with a maximum cooling power of 30.3 kW at 15 K [3].

The TMCP commissioning was completed independently, without connecting the CMS, in December 2022 [4-6]. Operational procedures, including cooldown, warm-up and beam injection modes, were thoroughly investigated to establish an automatic TMCP-CMS control system. In parallel, the CMS was installed into the Target building by January 2024. The first joint CMS-TMCP commissioning was conducted without the moderators connected, using nitrogen and helium as preliminary steps prior to hydrogen operation. The operational parameters of the CMS and TMCP during the cooldown and warm-up processes were analyzed based on the simulation results [7].

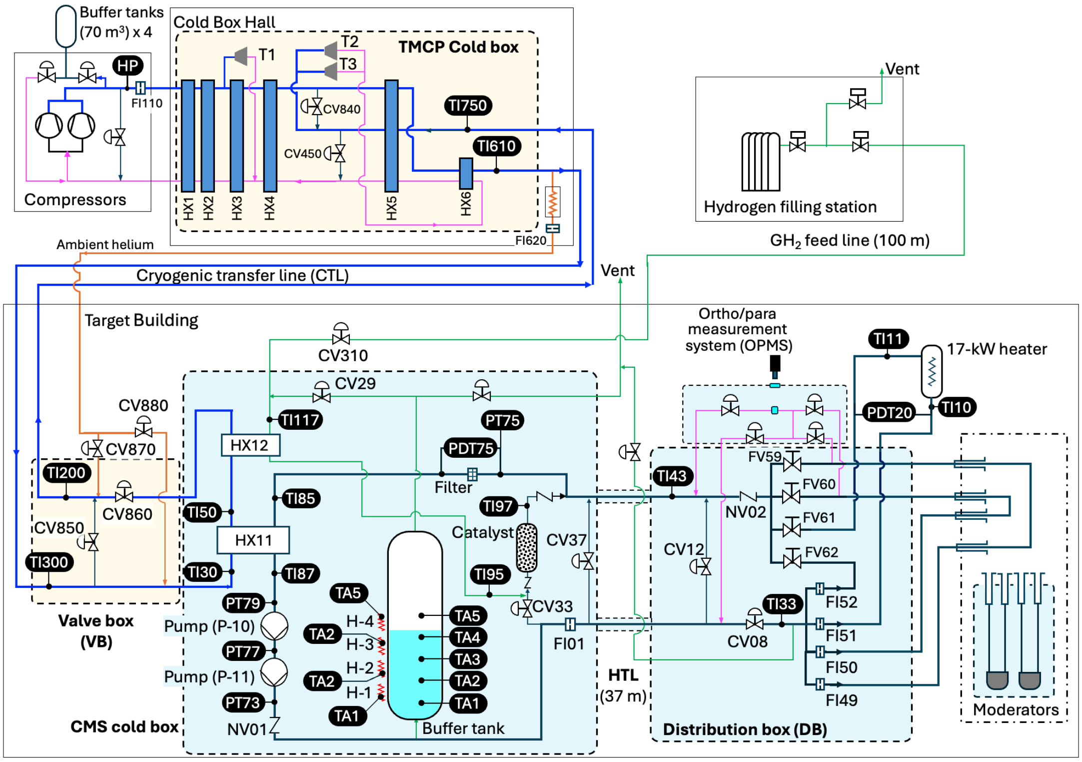

Figure 1. Overview of the ESS cryogenic moderator system (CMS).

Commissioning was suspended in May 2024 for the final installation of a 17-kW heater, designed to provide thermal compensation for nuclear heating.

From October to December 2024, CMS commissioning with helium resumed, bypassing the moderators. The CMS successfully cooled down to 17 K using the developed control units, while maintaining a pressure of 0.56 MPa. This ensured that the helium densities corresponded to those of gaseous hydrogen at the operational cooldown pressure of 1.1 MPa. Performance tests were carried out at 17 K, including measurements of pressure drops across the entire loop, evaluation of heat loads, liquid hydrogen pump performances, and testing of the 17-kW heater. This paper presents performance evaluation conducted during helium-based commissioning.

2. Commissioning of the CMS without connecting the moderators

2.1 Pressure drop measurement for each component

Figure 2 shows the measured pressure drops across the HX11 at 17.6 K and 0.63 MPa, obtained using the two pressure transmitters (PT79 and PT75). Prior to the cooldown, the pressure transmitters PT79 and PT75 were calibrated using PT77 as a reference. During the measurement, all bypass valves (CV37, CV33, and CV29) in the cold box were closed. The flow rate ($\dot{m}$) was measured by the orifice flow meter (FI01). The pressure drops were found to increase proportionally to the square of the mass flow rate. Tatsumoto et al. [8] reported that the pressure drop across equipment with complex geometries in turbulent flow regime can be expressed by a geometry-dependent parameter (F) as follows.

$$\Delta P = F\frac{\dot{m}^2}{\rho} \tag{1}$$

where $\dot{m}$ is the mass flow rate and ρ is the fluid density.

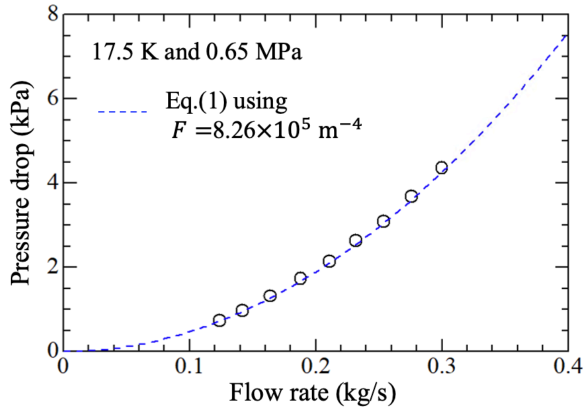

Figure 2. Pressure drops across the HX11.

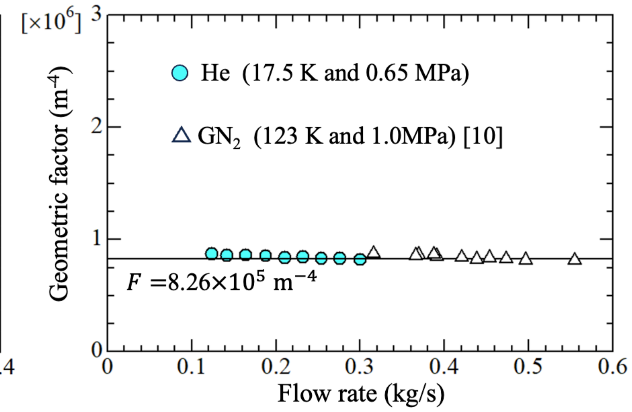

Figure 3. Geometric parameter of HX11.

Figure 3 shows the geometric parameter (F) derived from the pressure drops across the HX11. For comparison, value obtained during the prior commissioning using nitrogen at 120 K and 1.0 MPa [9] were also shown. The results demonstrate that the geometric parameter is consistent across different working fluids and can be expressed as 8.26×10^5 m^{-4}. The calculated pressure drops align with the measured values within an accuracy of $\pm$3%, as shown in Fig.2.

A 60 μm filter is located upstream of HX11 to protect the hydrogen pump impellers from debris and dust. A differential pressure transmitter (PDT75) is used to monitor debris accumulation on the filter. Figure 4 shows the geometric parameter derived from the pressure drop across the filter at 17.6 K and 0.63 MPa. The geometric parameter is represented by a consistent value of 1.55×10^6 m^{-4}, regardless of the working fluid. These results indicate that the filter can also function as a flow meter when this geometric parameter is applied. Figure 5 compares the flow rate estimated using the filter with that by the orifice flow meter. It was demonstrated that the filter-based flow measurement achieved an accuracy within $\pm$2%. This method allows the estimation of flow rates through HX11 and the pumps, independent of the positions of the bypass valves.

A 17-kW heater with a fast-response function was installed downstream of one of the return lines intended for future moderators. A differential pressure transmitter (PDT20) is installed to detect fluid instability that may occur due to boiling. Figure 6 shows the measured pressure drops across the heater at 17.6 K and 0.63 MPa, along with the corresponding geometric parameter. The results indicate that the geometric parameter was consistently represented by an identified value of 1.68×10^6 m^{-4} across the entire measurement range. The calculated pressure drops matched the measured pressure drop within an accuracy of $\pm$5%.

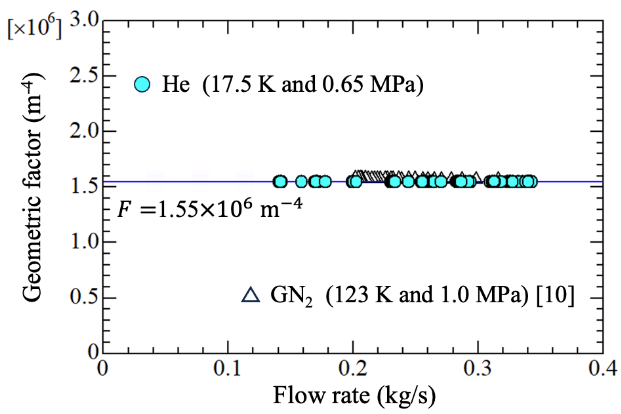

Figure 4. Geometric parameter of filter.

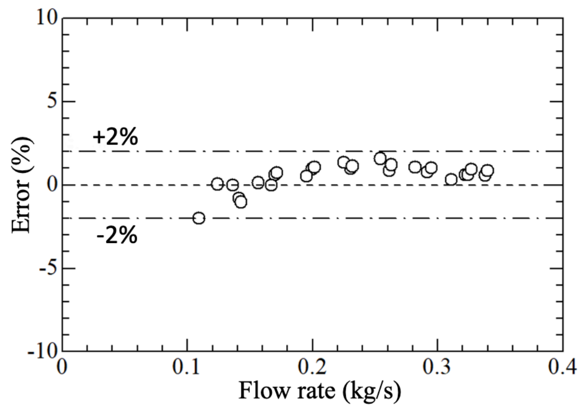

Figure 5. Flow rate estimated using the filter.

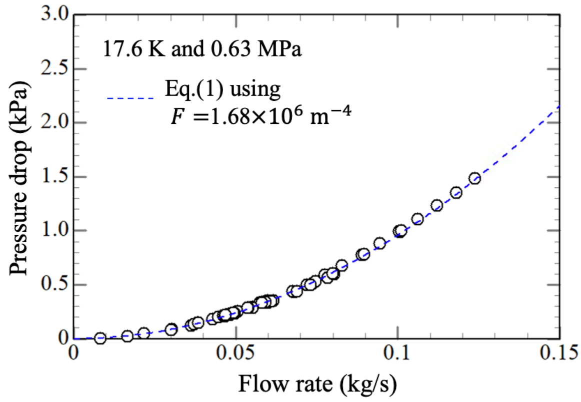

(a) Pressure drop

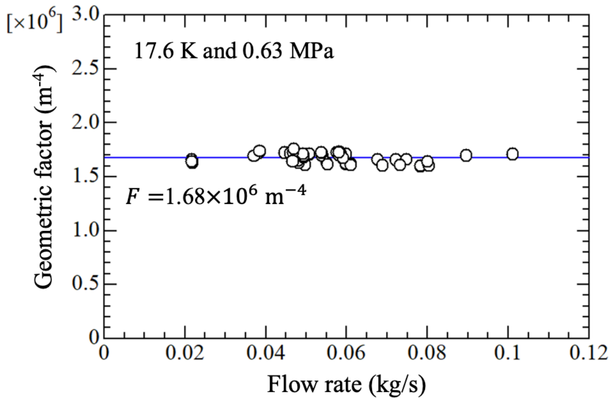

(b) Geometric factor

Figure 6. Pressure drops and geometric factor of the 17-kW heater.

2.2 Total pressure drop

Two ball-bearing-type centrifugal pumps arranged in series were designed to circulate liquid hydrogen at 17 K and 1.1 MPa. Each pump is equipped with a closed impeller, with a diameter (D) of 95.4 mm. The allowable revolution speed (N) ranges 1,000 to 14,000 rpm. The two pumps always operate at the same speed and can be considered as a single combined pump. The total pressure drop across the CMS loop is equivalent to the pump head of this combined pump (i.e., PT73—PT79). Figure 7 shows the measured total pressure drops across the CMS loop while varying the pump speed from 6,000 to 13,000 rpm, with CV08 to 100% and CV12 set to 10%. During the measurements, the other bypass valves in the cold box (CV29, CV33 and CV37) were temporarily closed. The predicted pump performances are also displayed in Fig. 7, along with pressure drops calculated using the simulation code by Tatsumoto et al. [7] under the same condition. The results demonstrate close agreement between the measured and calculated values, within 8% error.

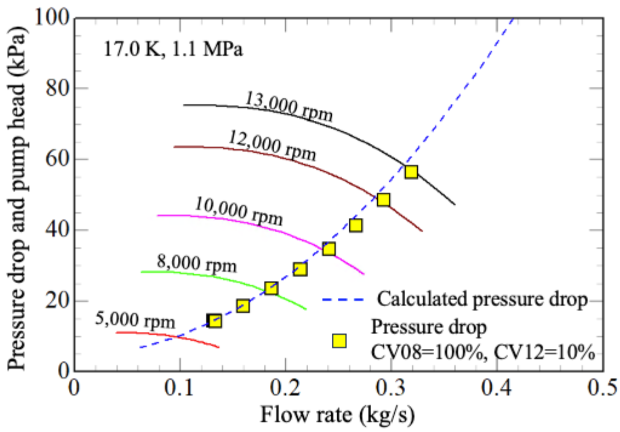

Figure 7. Measured total pressure drop on the predicted combined pump performance.

2.3 Heat load

According to the performance test results of hydrogen pump measured at 17.5 K and 0.61 MPa using helium [10], the maximum efficiency consistently occurred at a discharge coefficient of approximately 0.0292. The discharge coefficient (ϕ) is defined as follows.

$$\phi = \frac{\dot{m}}{\rho u_s D^2} \tag{2}$$

where $u_s = \pi ND/60$ is a wheel speed, ρ is the density, and $\dot{m}$ is the discharge mass flow rate.
It was observed that the side casing temperature (T_{ca}) in the vacuum chamber, as well as the pump flange temperature, decreased as the discharge coefficient deviated from 0.0292 at which the maximum efficiency (η_{max}) appeared. This behavior is attributed to flow-induced effect on the back side of the impeller. Figure 8 shows the heat loads (Q) measured at 16.6 K and 0.60 MPa by

varying the pump speeds from 6,000 to 13,000 rpm. During the measurement, CV12 and CV08 in the distribution box were adjusted to maintain the discharge coefficient at approximately 0.0292. The total heat loads were estimated using the inlet (TI85) and outlet (TI87) temperatures of the HX11. As the pump speeds increased, the heat loads also increased due to the rise in pump-generated heat. Consequently, the static heat load was estimated by subtracting the pump heat loads from the total heat load, resulting in an approximate value of 794 W.

2.4 Flow measurements

The CMS cold box includes three bypass lines, as shown in Fig.1: (1) a recondensation line for gaseous hydrogen from the pressure control buffer (PCB) tank via the second heat exchanger (HX12) and control valve (CV29), which reduces the CMS pressure; (2) a line for the ortho-to-parahydrogen catalyst vessel; and (3) a bypass line through the CMS cold box bypass via CV37. CV29 is operated using a PID controller to regulate the pressure (PT73), which is the highest pressure in the CMS loop. Excess hydrogen gas is recondensed via the HX12 and return to the pump suction through the catalyst vessel. A mass flow rate of 31.5 g/s through the catalyst vessel is required to ensure a parahydrogen fraction of more than 99.5% at the moderators [2]. This mass flow rate can be estimated indirectly if the flow rate through CV29 is known. The Kv values of CV29, specified as 1.1, were measured using the differential pressure transmitter at each valve position. During the measurement, helium was circulated at 17.5 K and 0.9 MPa, and the circulation flow rates were varied by changing the pump speed from 7,000 to 13,000 rpm. The bypass valve for the catalyst vessel (CV33) was closed. As described in 2.2, the filter was used as a flow meter ($\dot{m}_F$), utilizing the measured geometry factor of 1.55×10^{6} m^{-4}. The flow rates through CV29 were estimated by subtracting the flow rate

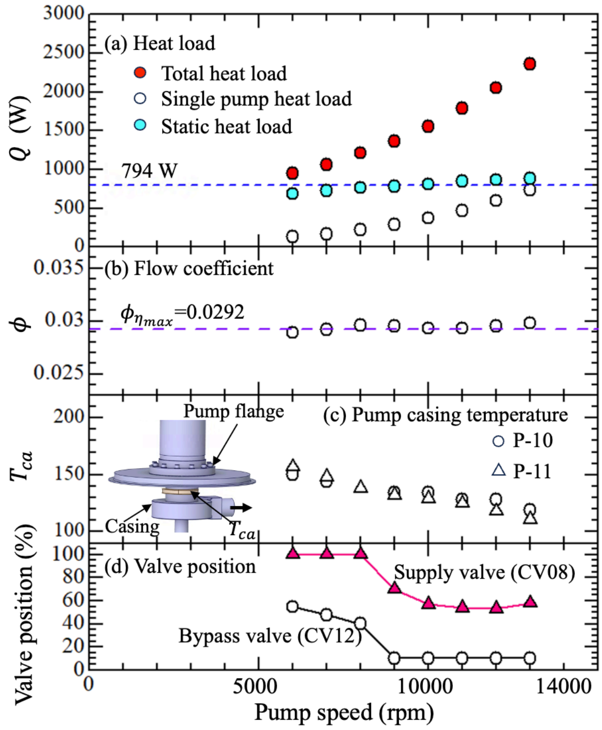

Figure 8. Heat load measurement results at 16.6 K and 0.6 MPa.

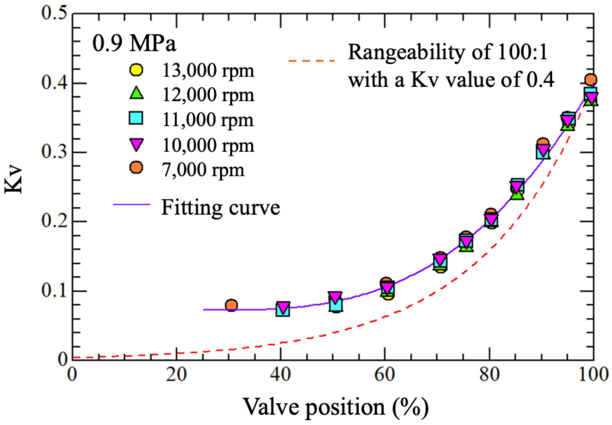

Figure 9. Measured Kv values of CV29.

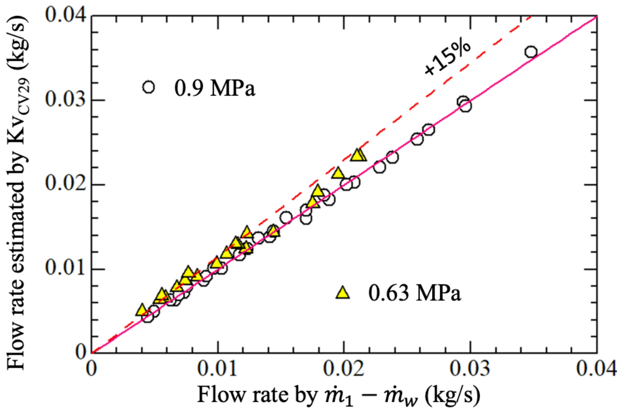

Figure 10. Verification of the calculated flow rate.

measured by FI01 ($\dot{m}$) from $\dot{m}_F$. Figure 9 shows the measured Kv values of CV29 at various valve positions at 0.9 MPa. The outlet temperatures of CV29 ranged from 22 to 26 K, depending on the valve position of CV29. The maximum measured Kv was 0.4, which was lower than the specified value of 1.1, when CV29 was fully open (100%). Due to the cracking pressure of the two check valves located at the inlet and outlet of the catalyst vessel, no flow was observed through the bypass line when the valve position was below 30%, and the Kv value approached 0.079. As the valve position decreased, the deviation from the Kv values estimated based on a rangeability of 100:1 increased due to the check valves. Based on the measurement data, the dependence of the Kv value on the valve position was determined using least squares fitting. Figure 10 compares the bypass flow rate calculated using the fitted Kv function with the estimated bypass flow rate ($\dot{m}_F - \dot{m}$). The results confirmed that the flow rate derived from the Kv value position relationship can be estimated within 15% error.

2.5 17 kW heater test

A high-power orifice-type heater with a fast-response function and a maximum power of 18 kW was designed to compensate for nuclear heating [11], based on the J-PARC heater developed by Tatsumoto et al. [12]. To achieve the required fast-response, 15 sheathed heater elements were directly exposed to the CMS process fluid. In May 2024, the heater was installed in one of the return lines designated for the future moderators, as shown in Fig. 1. The flow rate through the heater was regulated to 100 g/s by adjusting the positions of the return hand valves (FV59, FV60, FV61 and FV62). The heater powers, calculated from the phase voltage and heater element resistances, was gradually increased to 500W. Figure 11 presents the preliminary performance test results obtained at a flow rate of 100 g/s under the conditions of 17.6 K and 0.63 MPa. The measured heater power outputs were compared with the heat loads through the heater, which were estimated based on the temperature rise of TI11 at the heater outlet and the flow rate measured by the FI51 ($\dot{m}_{D2}$). Additionally, the heat loads were estimated using the temperature rise of TI85 at the HX11 inlet and the flow rate ($\dot{m}$). The results demonstrated that the heater power outputs showed good agreement between the heater power outputs and the estimated heat loads, within deviations of $\pm$10%.

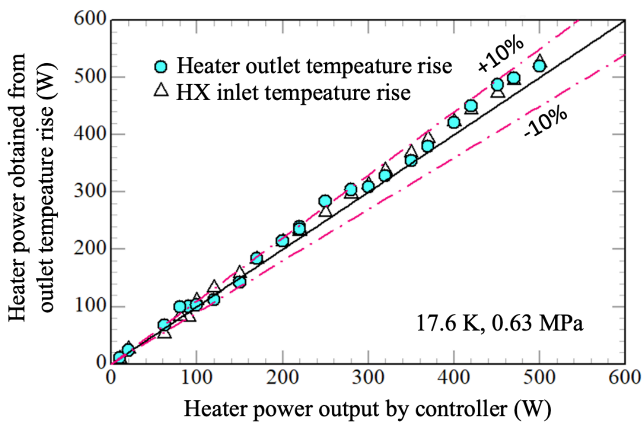

Figure 11. Preliminary performance test results of the heater.

Figure 12 shows the transient response test results for the heater as its power output increased from 100 W to 500 W at various power ramping speeds. The estimated travel time for helium to pass through the heater is 3.9 seconds, based on the heater's internal volume of 19 liters. At slow ramping speeds, the time delay between the heat power output and the corresponding heat load, estimated from the temperature rise of TI11 at the heater outlet, was approximately equal to the travel time. However, as the ramping speed increased, the time delay also increased. At a ramping speed of 400 W/s, the time delay extended to 5.9 seconds. The 3.9-second delay is attributed to the fluid residence time within the heater, while the additional 2.0-second delay is due to the time required for the heater to reach the corresponding temperature, which was influenced by its heat capacity. The results confirmed that the developed heater met the fast-response requirement.

IOP Conf. Series: Materials Science and Engineering **1344** (2026) 012042 doi:10.1088/1757-899X/1344/1/012042

The heater power was gradually increased to 450 W, and PID control was initiated with a setpoint of 18.5 K, as shown in Fig.13. The helium flow rate through the heater ($\dot{m}_{D2}$) was set to 129 g/s at 17.9 K and 0.6 MPa. Thermal fluctuations, resulting in a temperature rise of 0.13 K, were introduced by temporarily opening the bypass valve (CV12) from 10% to 50% for 16 seconds. The results confirmed that the PID control succcessfully regulated the outlet temperature to maintain the setpoint, although further tunning of the PID parameters is needed for the liquid hydrogen operation.

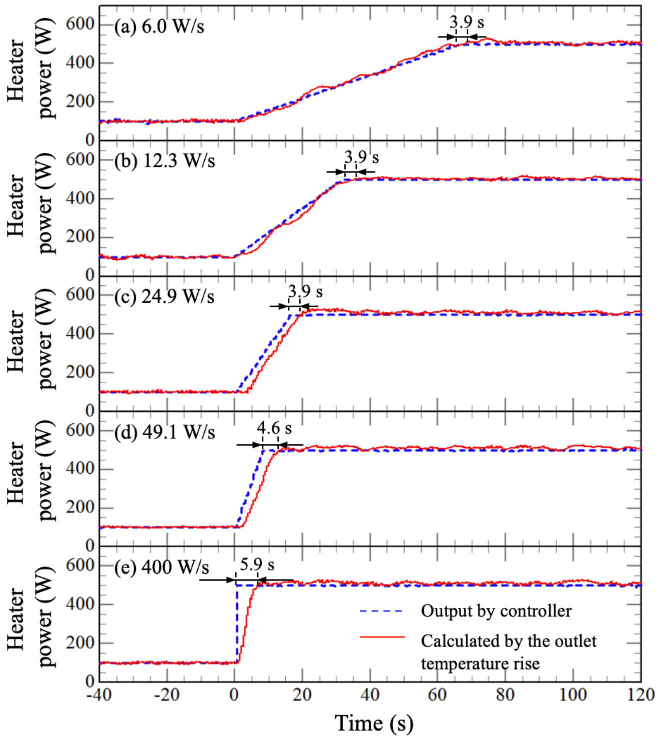

Figure 12. Transient response test results for the heater at 17.6 K and 0.63 MPa.

2.6 PCB band heater test

Four band heaters, each with a height of 53 mm and a capacity of 500 W, were wrapped around the side of the pressure control buffer (PCB) tank, which has a diameter of 300 mm and volume of 71 liters. The corresponding heat flux is 1.0×10^4 W/m^2 at 500W. Copper wool was inserted between the band heaters and the PCB tank to improve thermal contact [11]. A Pt100 temperature sensor is mounted on each band heater to protect overheating. For this preliminary heater test, the pump speed was increased to 12,000 rpm at 0.62 MPa to achieve a higher pump head, thereby enhancing the bypass flow rate via CV29, which was set to 100% open to maximize the flow rate through the PCB tank. The catalyst bypass valve (CV33) remained fully closed. Figure 14 presents the heater test results, where the second (H-2), third (H-3) and fourth (H-4) heaters from the bottom were used. During the measurement, the flow rate through the PCB tank, calculated as $\dot{m}_F - \dot{m}$, was maintained at 22 g/s. The total heater power was gradually increased to 286 W (94 W per heater), and the temperatures of individual heaters were monitored. Due to signal conditioner limitations, temperatures below 73 K could not be measured by Pt100. Unlike the 17-kW heater described in 2.6, the temperature behaviour of H-3 indicated that it took more than 500 seconds to stabilize when 94 W of power was applied. Heat load calculations obtained from the flow rate $(\dot{m}_F - \dot{m})$ and the

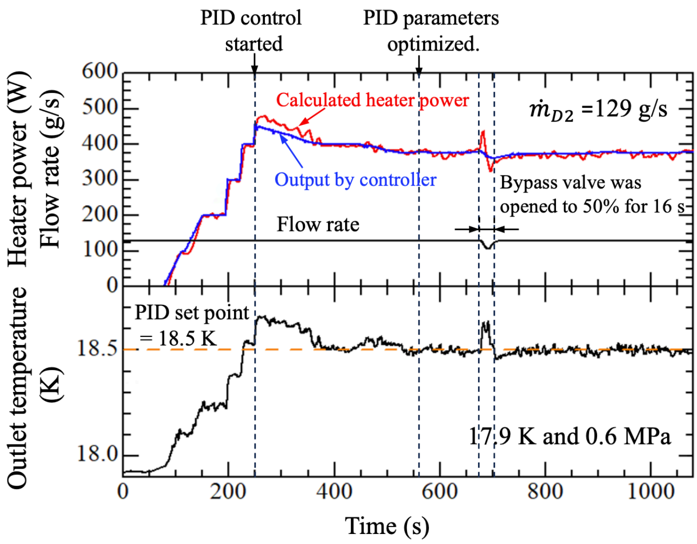

Figure 13. Test results for the heater PID control.

temperature difference between T117 at CV29 and TA1 at the bottom of the PCB tank were in good agreement with the heater power outputs, within 8% errors. Although the band heaters were originally designed for use with liquid hydrogen to facilitate evaporation and increase system pressure, the results demonstrated that they could also be used with gaseous hydrogen. This is feasible because gaseous hydrogen provides better heat transfer than gaseous helium, provided that the heater power is limited to 94 W. Moreover, the results validated the reliability and practicality of the flow rate estimation method using $\dot{m}_F - \dot{m}$.

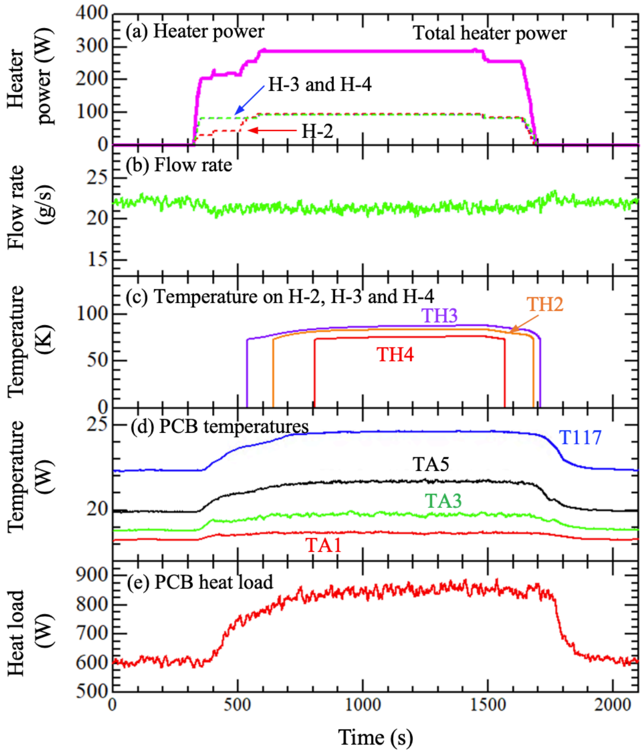

Figure 14. PCB heater test results at 17.4 K and 0.62

3. Conclusions

The CMS installation has been completed in May 2024. Commissioning was subsequently carried out using helium, without connecting the moderators, as a preparatory step for hydrogen operation. During this phase, performance tests were conducted on the hydrogen pumps, the 17-kW fast-response heater, the band heaters on the PCB tank for the CMS pressure adjustment. In addition, pressured drop and heat load measurements were performed. The test results confirmed that the system performances met the design requirements.

References

[1] Bessler Y, Henkes C, Hanusch F, Schumacher P, Natour G, Butzek M, Klaus M, Lyngh D and Kickulies M 2017 *IOP Conf. Ser: Materials Science and Engineering* **171** (2017) 012131.

[2] Tatsumoto H, Lyngh D, Bessler Y, M Klaus, Hanusch F, P Arnold and H Quack *IOP Conf. Ser: Materials Science and Engineering* **755** (2019) 012101.

[3] Arnold P, Hess W, Jurns J, Su X T, Wang X L and Weisend II J G 2015 *IOP Conf. Ser: Materials Science and Engineering* **101** 012011.

[4] Tatsumoto H, Arnold P, Boros M and Horvath A 2024 *IOP Conf. Ser.: Mater. Sci. Eng* ***1301*** *1131.*

[5] Tatsumoto H, Arnold P, Boros M and Horvath A 2024 *IOP Conf. Ser.: Mater. Sci. Eng* ***1301*** *1126.*

[6] Tatsumoto H, Arnold P, Boros M and Horvath A 2024 *IOP Conf. Ser.: Mater. Sci. Eng* ***1301*** *1123.*

[7] Tatsumoto H, Arnold P, Boros M and Horvath A 2024 *IOP Conf. Ser.: Mater. Sci. Eng* ***1301*** *1086.*

[8] Tatsumoto H, Aso T, Kato T, Ohtsu K, Maekawa F, Kato T, Futakawa F 2010 *Advances in Cryogenic Engineering* **55** 1162-1169.

[9] Tatsumoto H, Horvath A, , Arnold P, Segerup M, Tereszkowski P, Arriagada J 2025 *IOP Conf. Ser.: Mater. Sci. Eng* ***1327*** *012032.*

[10] Tatsumoto H, Horvath A, Vasilopoulos T, Haag I, Ariyoshi G, "Performance assessment of liquid hydrogen pump for the ESS cryogenic moderator system during initial commissioning using helium", presented in CEC-ICMC 2025 (C2Po1A-05), submitted to *Advances in Cryogenic Engineering* (at press).

[11] Tatsumoto H, Horvath A, Tereszkowski P, Segerup M, Arnold P Bessler Y Peter R, Derking H, "Updated design of the ESS cryogenic moderator system", presented in CEC-ICMC 2025 (C1Po1A-06), submitted to *Advances in Cryogenic Engineering* (at press).

[12] Tatsumoto H, Aso T, Kato T, Ohtsu K, Maekawa F, Futakawa F, *Cryogenics* **51**, (2010) 315-320.